Generalized diffusion model in optical tomography with clear layers

Guillaume Bal and Kui Ren *

July 15, 2003

Abstract

We introduce a generalized diffusion equation that models the propagation of photons in highly scattering domains with thin non-scattering clear layers. Classical diffusion models break down in the presence of clear layers. The model we propose in this paper accurately accounts for the clear layer effects and has a comparable computational cost to classical diffusion. It is based on modeling the propagation in the clear layer as a local tangential diffusion process. It can be justified mathematically in the limit of small mean-free-paths and is shown numerically to be very accurate in two and three dimensional idealized cases. We believe that this model can be used as an accurate forward model in optical tomography.

1 Introduction

Optical tomography is increasingly being used as a medical imaging tool to assess the scattering and absorbing properties of human tissues probed by near-infra-red photons. Several works [1, 2, 3, 4, 5, 6, 7, 8] exist on the practical, theoretical, and computational aspects of optical tomography. Among other applications, optical tomography is being considered as an interesting technique to image tumors and monitor cerebral oxygenation in neonates. This is the application of interest in this paper.

Photon propagation in human tissues is best modeled by a radiative transport equation that describes the density of photons in the phase space, i.e., as a function of position and direction. Such models are quite expensive computationally although they are being used more and more often recently [9]. This is the reason why an approximation to radiative transport is often preferred. It takes the form of a diffusion equation, which only models photon density spatially. The regime of validity of diffusion has been extensively studied [1, 10, 11]. Essentially diffusion can be used when tissue scattering is high and absorption small. Such assumptions are verified by almost all human tissues in the head but for a thin layer filled with cerebrospinal fluid. This layer is almost collision-less and absorption-less. Diffusion models perform very poorly in such layers [12, 13, 14, 15]. These models have to be modified if one wants to image the oxygenation in the head of neonates for instance.

One could certainly solve phase-space transport equations instead of the inaccurate diffusion equations [12, 16]. There exists a large literature on numerical techniques that allow us to use coarser schemes (modeling transport or diffusion equations) in the regions where multiple scattering makes the simulation relatively straightforward and finer schemes in the vicinity of the clear layer where transport effects must be calculated accurately [17, 18, 19, 20, 21].

Because clear layers are thin in practice, an alternative solution exists to solving transport equations. A lot of work has been done by Arridge and his collaborators to develop hybrid models that would solve a diffusion equation where the tissues are highly scattering and model the transport behavior in the clear layer [13, 14, 15]. Similar models were developed using an approach based on the asymptotic expansion of transport equations by one of the authors [22, 23]. The models that come out of this research have the following common features. 1) They are diffusion equations with matching conditions at the boundary of

*Department of Applied Physics and Applied Mathematics, Columbia University, New York NY, 10027

the layer that account for the guiding effect of the clear layer. 2) These matching conditions take the form of non-local interface conditions for the photon density and current. 3) These models are quite accurate in practice, both to solve forward and inverse problems. 4) Their computational cost is much lower than that of full transport. 5) However it is often significantly higher than the cost of classical diffusion and the models are quite complicated to implement in practice.

In this paper we build on the asymptotic expansion techniques [22, 23] to propose a new model that accurately models the clear layer effects for a computational cost and an implementation by finite element method that is essentially the same as that of classical diffusion. The model is obtained by localizing the interface conditions at the clear layer. This local interface condition models a tangential diffusion process that accounts for the propagation of photons along the clear layer. In variational form, this diffusion process is about as easy to solve as the classical volume diffusion process.

The rest of the paper is structured as follows. Section 2 recalls some results on the transport and classical diffusion models. Section 3 presents the new generalized diffusion model with local interface conditions. Explicit expressions are obtained for the tangential diffusion equation in the case of two dimensional circular clear layers. Section 4 confirms numerically the accuracy of the model in the idealized cases of circular clear layers within the unit disc in a two-dimensional setting and spherical clear layers within the unit sphere in a three-dimensional setting. Section 5 offers some conclusions.

2 Transport and Diffusion models

We model photon propagation in human tissues by the following steady-state linear radiative transfer equation

$$\begin{aligned} &\mathbf{\Omega}\cdot\nabla u(\mathbf{x},\mathbf{\Omega})+\sigma_a(\mathbf{x})u(\mathbf{x},\mathbf{\Omega})+Q(u)(\mathbf{x},\mathbf{\Omega})=S(\mathbf{x}), \qquad \text{in } \mathcal{D}\times S^{n-1}\\ &u(\mathbf{x},\mathbf{\Omega})=g(\mathbf{x},\mathbf{\Omega}) \qquad \text{on } \Gamma_-=\{(\mathbf{x},\mathbf{\Omega})\in\partial\mathcal{D}\times S^{n-1} \text{ s.t. } \mathbf{\Omega}\cdot\boldsymbol{\nu}(\mathbf{x})<0\}. \end{aligned} \tag{1}$$

Here, $u(\mathbf{x},\mathbf{\Omega})$ is the photon flux intensity at point $\mathbf{x}\in\mathcal{D}$, where $\mathcal{D}$ is a subset in $\mathbb{R}^n$, with direction of propagation $\mathbf{\Omega}\in S^{n-1}$, where S^{n-1} is the unit sphere in $\mathbb{R}^n$. The space dimension is $n=3$ in practice. In this paper we consider $n=2$ because it is computationally simpler and $n=3$. The source of photons at the boundary of the domain is given by $g(\mathbf{x},\mathbf{\Omega})$ and the outward unit normal to the domain is $\boldsymbol{\nu}(\mathbf{x})$ at $\mathbf{x}\in\partial\mathcal{D}$. The volume source of photons is given by $S(\mathbf{x})$. The absorption coefficient is denoted by $\sigma_a(\mathbf{x})$, and the scattering operator Q is defined as

$$Q(u)(\mathbf{x},\mathbf{\Omega})=\sigma_s(\mathbf{x})\Big(u(\mathbf{x},\mathbf{\Omega})-\int_{S^{n-1}}u(\mathbf{x},\mathbf{\Omega}')d\mu(\mathbf{\Omega}')\Big). \tag{2}$$

Here, $\sigma_s(\mathbf{x})$ is the scattering coefficient and $d\mu$ is the surface measure on S^{n-1} normalized so that $\int_{S^{n-1}}d\mu(\mathbf{\Omega})=1$.

In two space dimensions, we parameterize $\mathbf{\Omega}=(\cos\theta,\sin\theta)$ and have

$$\int_{S^1}u(\mathbf{x},\mathbf{\Omega})d\mu(\mathbf{\Omega})=\frac{1}{2\pi}\int_0^{2\pi}u(\mathbf{x},\theta)d\theta,$$

identifying $u(\mathbf{x},\mathbf{\Omega})$ with $u(\mathbf{x},\theta)$. In three space dimensions, we parameterize $\mathbf{\Omega}=(\sin\theta\cos\phi,\sin\theta\sin\phi,\cos\theta)$ and have

$$\int_{S^2}u(\mathbf{x},\mathbf{\Omega})d\mu(\mathbf{\Omega})=\frac{1}{4\pi}\int_0^{2\pi}\int_0^{\pi}u(\mathbf{x},\theta,\phi)\sin\theta d\theta d\phi,$$

identifying $u(\mathbf{x},\mathbf{\Omega})$ with $u(\mathbf{x},\theta,\phi)$.

The optical tomography problem consists of reconstructing $\sigma_a(\mathbf{x})$ and $\sigma_s(\mathbf{x})$ from boundary measurements $u(\mathbf{x},\mathbf{\Omega})$ for $\mathbf{x}\in\partial\mathcal{D}$ and $\mathbf{\Omega}\in S^{n-1}$. This is quite a difficult problem both in theory and in practice [1, 3, 6, 24, 9, 25]. This problem is also very expensive computationally because the radiative transfer equations are posed in the phase space, with a minimum of three spatial variables and two angular variables in practical calculations. They are therefore often replaced by their diffusion approximation, which does not involve any angular variable.

Diffusion approximations are valid in the regime of high scattering $\sigma_s \gg 1$ and small absorption $\sigma_a \ll 1$. We can then approximate the solution $u(\mathbf{x}, \mathbf{\Omega})$ by

$$u(\mathbf{x}, \mathbf{\Omega}) = U(\mathbf{x}) - \frac{1}{\sigma_s(\mathbf{x})}\mathbf{\Omega} \cdot \nabla U(\mathbf{x}) + \text{ smaller order terms,} \tag{3}$$

where $U(\mathbf{x})$ is the solution to the following diffusion equation

$$\begin{aligned} -\nabla \cdot D(\mathbf{x})\nabla U(\mathbf{x}) + \sigma_a(\mathbf{x})U(\mathbf{x}) = S(\mathbf{x}) \qquad & \text{in } \mathcal{D} \\ U(\mathbf{x}) + nL_n D(\mathbf{x})\boldsymbol{\nu}(\mathbf{x}) \cdot \nabla U(\mathbf{x}) = g(\mathbf{x}) \qquad & \text{on } \partial\mathcal{D}, \end{aligned} \tag{4}$$

where we assume that $g(\mathbf{x}, \mathbf{\Omega}) = g(\mathbf{x})$ does not depend on $\mathbf{\Omega}$ to simplify, and were the diffusion coefficient is defined by

$$D(\mathbf{x}) = \frac{1}{n\sigma_s(\mathbf{x})}, \qquad n = 2, 3. \tag{5}$$

The extrapolation length L_n accounts for the leakage of photons at the domain boundary. Approximate values are $L_2 = 0.8164$ and $L_3 = 0.7104$ for isotropic scattering [10, 22, 26, 27]. Diffusion equations are very well studied both mathematically and physically and can be justified by various means [1, 10, 11].

The diffusive regime is valid in most human tissues, where absorption is relatively small and scattering quite large, with typical values of the order of $\sigma_a = 0.1\text{cm}^{-1}$ and $\sigma_s = 20\text{cm}^{-1}$. This correspond to an absorption mean free path of 10cm and a scattering mean free path of 0.05cm. Notice that $D(\mathbf{x})$ and $\sigma_a(\mathbf{x})$ in (4) are then of comparable order.

The presence of cerebrospinal fluid in the human head prevents the use of the classical diffusion equation (4). The reason is that this fluid is optically clear: photons propagate along straight lines almost scattering-free in such fluids. This creates a guiding effect that the diffusion equation (4) cannot capture. Several works exist to understand and fix this problem [13, 14, 22, 23, 28]. The main idea consists of using the diffusion equation where it is valid and coupling it with local transport in the non-scattering regions. An asymptotic analysis [23] justifies such an approach for thin clear inclusions. Several such hybrid models have been analyzed numerically [22]. This analysis shows the adequacy and robustness of the models. The main difficulty is that their numerical implementation is still difficult and their cost significantly higher than that of classical diffusion (4), although much lower than that of the full transport equation (1). It is the objective of this paper to further simplify the hybrid model and obtain a scheme that is both accurate and computationally efficient.

3 Generalized diffusion model

Following an earlier asymptotic derivation [23], we propose here what we believe is the simplest model that captures both the diffusive behavior outside of the clear layer and the guiding effect within the clear layer. It is based on solving a diffusion equation with local jump conditions at the clear layer.

3.1 Notation and Geometry.

The geometry of the clear layer $\mathcal{D}^C$ is as follows. We define Σ as a closed smooth surface embedded in $\mathcal{D}$ and

$$\mathcal{D}^C = \{\mathbf{y} \in \mathcal{D} \text{ s.t. } \mathbf{y} = \mathbf{x} + t\boldsymbol{\nu}(\mathbf{x}), \quad \text{where } \mathbf{x} \in \Sigma \text{ and } |t| < L\}. \tag{6}$$

Here L is a fixed sufficiently small number and $\boldsymbol{\nu}(\mathbf{x})$ is the outward normal to (the volume inside) Σ at $\mathbf{x} \in \Sigma$. We denote by Σ^E and Σ^I the outer and inner surfaces of $\mathcal{D}^C$ and assume that these surfaces are smooth; see Fig. 1. We define $\boldsymbol{\nu}_C(\mathbf{x})$ as the outward unit normal to $\mathcal{D}^C$ at a point $\mathbf{x} \in \partial\mathcal{D}^C = \Sigma^E \cup \Sigma^I$. For $\mathbf{x} \in \Sigma$, we define

$$\mathbf{x}^E = \mathbf{x} + L\boldsymbol{\nu}(\mathbf{x}) \in \Sigma^E \qquad \text{and} \qquad \mathbf{x}^I = \mathbf{x} - L\boldsymbol{\nu}(\mathbf{x}) \in \Sigma^I. \tag{7}$$

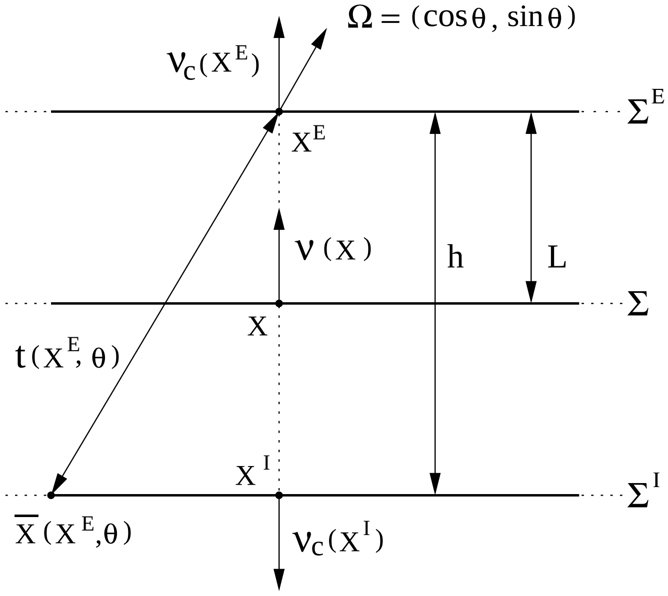

Figure 1: Local Geometry of the clear layer.

It is useful to see $\mathbf{x}^E$ and $\mathbf{x}^I$ as functions of $\mathbf{x} \in \Sigma$. Notice that the outward normal to $\mathcal{D}^C$ at $\mathbf{x}^E \in \Sigma^E$ is $\boldsymbol{\nu}_C(\mathbf{x}^E) = \boldsymbol{\nu}(\mathbf{x})$ and the outward normal at $\mathbf{x}^I \in \Sigma^I$ is $\boldsymbol{\nu}_C(\mathbf{x}^I) = -\boldsymbol{\nu}(\mathbf{x})$.

The solution operator to the radiative transfer equation in $\mathcal{D}^C$ is denoted by $\mathcal{R}^C$. Let us define

$$\Gamma^C_\pm = \{(\mathbf{x}, \boldsymbol{\Omega}) \in \partial\mathcal{D}^C \times S^{n-1} \text{ s.t. } \pm\boldsymbol{\Omega}\cdot\boldsymbol{\nu}_C(\mathbf{x}) > 0\},$$

and consider the problem inside the layer

$$\begin{aligned} &\boldsymbol{\Omega}\cdot\boldsymbol{\nabla} v(\mathbf{x},\boldsymbol{\Omega}) + \sigma_a(\mathbf{x})v(\mathbf{x},\boldsymbol{\Omega}) + Q(v)(\mathbf{x},\boldsymbol{\Omega}) = 0, \qquad \text{in } \mathcal{D}^C \times S^{n-1} \\ &v(\mathbf{x},\boldsymbol{\Omega}) = g(\mathbf{x},\boldsymbol{\Omega}) \quad \text{ on } \Gamma^C_-. \end{aligned}$$

We then define $\mathcal{R}^C$ as the operator that maps $g(\mathbf{x},\boldsymbol{\Omega})$ on Γ^C_- to $v(\mathbf{x},\boldsymbol{\Omega})|_{\Gamma^C_+} = \mathcal{R}^C g(\mathbf{x},\boldsymbol{\Omega})$, the restriction to the transport solution $v(\mathbf{x},\boldsymbol{\Omega})$ to the outgoing surface (in the phase space) Γ^C_+. Such an operator is well defined in suitably chosen weighted L^p spaces [10].

We now define the operator $\mathcal{R}^C_1$ by

$$\mathcal{R}^C_1 = \mathcal{R}^C - \mathcal{I}, \tag{8}$$

where the near-identity operator $\mathcal{I}$ is defined from Γ^C_- to Γ^C_+ by

$$\mathcal{I}u(\mathbf{x},\boldsymbol{\Omega}) = \begin{cases} u(\mathbf{x} + 2L\boldsymbol{\nu}(\mathbf{x}), \boldsymbol{\Omega}), & \text{when } \mathbf{x} \in \Sigma^I \\ u(\mathbf{x} - 2L\boldsymbol{\nu}(\mathbf{x}), \boldsymbol{\Omega}), & \text{when } \mathbf{x} \in \Sigma^E. \end{cases}$$

This near-identity operator $\mathcal{I}$ is merely a translation from the inner boundary to the outer boundary and vice versa. This is an approximation to what happens to most photons that cross the clear layer: since the clear layer is optically thin (because σ_s is small in $\mathcal{D}^C$) and most photons reach the clear layer at $\mathbf{x}^I$ with an incidence angle far from orthogonal to $\boldsymbol{\nu}(\mathbf{x})$, they do not propagate for a long time in the clear layer and exit it at a point near $\mathbf{x}^E$. For those relatively rare photons that reach the clear layer with a direction almost orthogonal to $\boldsymbol{\nu}(\mathbf{x})$, the exit point will no longer be $\mathbf{x}^E$. This behavior is captured by $\mathcal{R}^C_1$ and modifies the local current equilibrium.

3.2 Generalized diffusion equation with non-local interface conditions.

It was shown [23, p.1687] that a good approximation of $u(\mathbf{x}, \mathbf{\Omega})$, the solution to (1), was given by $U(\mathbf{x})$ solution of

$$\begin{aligned}
&-\nabla \cdot D(\mathbf{x})\nabla U(\mathbf{x}) + \sigma_a(\mathbf{x})U(\mathbf{x}) = S(\mathbf{x}) \qquad \text{in } \mathcal{D}\backslash\mathcal{D}^C \\
&U(\mathbf{x}) + nL_n D(\mathbf{x})\boldsymbol{\nu}(\mathbf{x}) \cdot \nabla U(\mathbf{x}) = g(\mathbf{x}) \qquad \text{on } \partial\mathcal{D} \\
&U(\mathbf{x}^E) = U(\mathbf{x}^I) \qquad \text{on } \Sigma \\
&\boldsymbol{\nu}(\mathbf{x}) \cdot D(\mathbf{x}^E)\nabla U(\mathbf{x}^E) - \boldsymbol{\nu}(\mathbf{x}) \cdot D(\mathbf{x}^I)\nabla U(\mathbf{x}^I) = KU(\mathbf{x}) \text{ on } \Sigma,
\end{aligned} \tag{9}$$

where the integral operator K is given by

$$\begin{aligned}
KU(\mathbf{x}) &= \int_{\Gamma_+(\mathbf{x}^E)} \mathbf{\Omega} \cdot \boldsymbol{\nu}_C(\mathbf{x}^E)(\mathcal{R}_1^C U)(\mathbf{x}^E, \mathbf{\Omega})d\mu(\mathbf{\Omega}) \\
&+ \int_{\Gamma_+(\mathbf{x}^I)} \mathbf{\Omega} \cdot \boldsymbol{\nu}_C(\mathbf{x}^I)(\mathcal{R}_1^C U)(\mathbf{x}^I, \mathbf{\Omega})d\mu(\mathbf{\Omega}).
\end{aligned} \tag{10}$$

We have defined $\Gamma_+(\mathbf{x}) = \{\mathbf{\Omega} \in S^{n-1} \text{ s.t. } \mathbf{\Omega} \cdot \boldsymbol{\nu}_C(\mathbf{x}) > 0\}$ and have implicitly used that $\mathbf{x}^E$ and $\mathbf{x}^I$ defined in (7) are functions of $\mathbf{x} \in \Sigma$. Notice that this diffusion problem is posed on $\mathcal{D}\backslash\mathcal{D}^C$. What happens inside the layer $\mathcal{D}^C$ is modeled by the operator $\mathcal{R}_1^C$ in the definition of K. The two jump conditions in (9) indicate the boundary conditions satisfied by U at the boundary $\partial\mathcal{D}^C$. It was shown [23] that the above problem (9) was well-posed provided that the thickness of the layer L was sufficiently small. Numerical simulations based on (9) and on similar generalized diffusion models [22, 23] have shown the accuracy of the approximation.

The physical interpretation of the jump conditions is the following. The jump of the total flux vanishes, $U(\mathbf{x}^E) = U(\mathbf{x}^I)$, because the clear layer is not sufficiently thick to modify this equilibrium. However, it is sufficiently large to modify the current balance. The difference of currents crossing the interfaces of the clear layer is balanced by the current of photons inside the clear layer. The latter is modeled by $KU(\mathbf{x})$. As a minor remark, let us mention that the asymptotic expansion [23] involves an additional Jacobian term corresponding to the map $\mathcal{I}$. Since $\mathcal{I}$ is near-identity, we have replaced the Jacobian by 1. Accounting for this Jacobian does not change the limiting equations that will be obtained below.

3.3 Localization of the interface conditions.

We now aim at further simplifying (9) by replacing the nonlocal operator K in (10) by its local approximation. In doing so, we will model the clear layer $\mathcal{D}^C$ by a local jump condition for the diffusion solution at Σ. We assume that the clear layer is totally non-scattering, i.e. that $\sigma_s(\mathbf{x}) = 0$ for $\mathbf{x} \in \mathcal{D}^C$. This assumption is fairly accurate in practice. All the results we present below are not significantly modified when the layer is weakly scattering; see our remarks at the end of the section.

Let us consider the two-dimensional case $n = 2$. Let $(\mathbf{x}, \mathbf{\Omega}) \in \Gamma_+^C$. We define $t(\mathbf{x}, \theta)$ as the time it takes to travel from Γ_-^C to $\mathbf{x}$ in direction $-\mathbf{\Omega}$ (with unit speed). We also define $\overline{\mathbf{x}} = \overline{\mathbf{x}}(\mathbf{x}, \theta) = \mathbf{x} - t(\mathbf{x}, \theta)\mathbf{\Omega}$, the starting point on Γ_-^C. Since the clear layer is non-scattering, we obtain by solving the free transport equation along its characteristics that

$$\mathcal{R}^C U(\mathbf{x}, \theta) = e^{-\sigma_a t(\mathbf{x}, \theta)} U(\overline{\mathbf{x}}),$$

assuming that absorption is constant in $\mathcal{D}^C$. Let us consider a point $\mathbf{x}^I \in \Sigma^I$ such that $\overline{\mathbf{x}}(\mathbf{x}^I, \theta) \in \Sigma^E$ for all θ such that $\boldsymbol{\nu}_C(\mathbf{x}^I) \cdot \mathbf{\Omega} > 0$. This means that the photons reaching $\mathbf{x}^I$ all come from the other interface Σ^E. We then have that the contribution to the current of photons crossing Σ^I is given by

$$\begin{aligned}
J^I &= \int_{\Gamma_+(\mathbf{x}^I)} \mathbf{\Omega} \cdot \boldsymbol{\nu}_C(\mathbf{x}^I)(\mathcal{R}_1^C U)(\mathbf{x}^I, \mathbf{\Omega})d\mu(\mathbf{\Omega}) \\
&= \frac{1}{2\pi} \int_0^\pi \sin\theta \Big(e^{-\sigma_a t(\mathbf{x}^I, \theta)} U(\overline{\mathbf{x}}^I) - U(\mathbf{x}^E) \Big) d\theta,
\end{aligned}$$

where θ is chosen so that $0 \leq \theta \leq \pi$ spans $\Gamma_-^C(\mathbf{x}^I)$. Notice that both $\overline{\mathbf{x}}^I$ and $\mathbf{x}^E$ belong to Σ^E. Locally around $\mathbf{x}^E$ we can parameterize Σ^E by the arc-length distance $s(\overline{\mathbf{x}}^I) \equiv s(\theta, \mathbf{x}^E)$ to $\mathbf{x}^E$. When the curvature of Σ is positive, all points $\overline{\mathbf{x}}^I$ are close to $\mathbf{x}^E$ since the clear layer is thin. We can thus use the Taylor expansion

$$\begin{aligned} U(\overline{\mathbf{x}}^I) &= U(\mathbf{x}^E) + s(\theta;\mathbf{x}^E)\frac{\partial U}{\partial s}(\mathbf{x}^E) + \frac{1}{2}s^2(\theta;\mathbf{x}^E)\frac{\partial^2 U}{\partial s^2}(\mathbf{x}^E) + \text{ smaller terms} \\ &= U(\mathbf{x}^E) + \frac{\partial}{\partial s}\Big(\frac{s^2(\theta;\mathbf{x}^E)}{2}\frac{\partial U}{\partial s}\Big)(\mathbf{x}^E) + \text{ smaller terms.} \end{aligned} \tag{11}$$

Similarly, we have

$$e^{-\sigma_a t(\mathbf{x}^I,\theta)} = 1 - \sigma_a t(\mathbf{x}^I,\theta) + \text{ smaller terms.} \tag{12}$$

We finally obtain the following approximation

$$\begin{aligned} J^I &= -\sigma_a^I(\mathbf{x}^I)U(\mathbf{x}^E) + b^I(\mathbf{x}^E)\frac{\partial U}{\partial s}(\mathbf{x}^E) + d^I(\mathbf{x}^E)\frac{\partial^2 U}{\partial s^2}(\mathbf{x}^E) + \dots \\ &= -\sigma_a^I(\mathbf{x}^I)U(\mathbf{x}^E) + \frac{\partial}{\partial s}\Big(d^I(\mathbf{x}^E)\frac{\partial U}{\partial s}\Big)(\mathbf{x}^E) + \dots, \end{aligned} \tag{13}$$

where

$$\begin{aligned} \sigma_a^I(\mathbf{x}^I) &= \sigma_a \frac{1}{2\pi}\int_0^\pi t(\mathbf{x}^I,\theta)\sin\theta d\theta \\ b^I(\mathbf{x}^E) &= \frac{1}{2\pi}\int_0^\pi s(\theta;\mathbf{x}^E)\sin\theta d\theta \\ d^I(\mathbf{x}^E) &= \frac{1}{2\pi}\int_0^\pi \frac{1}{2}s^2(\theta;\mathbf{x}^E)\sin\theta d\theta. \end{aligned} \tag{14}$$

Notice that b^I vanishes when the surface Σ is symmetrical about $\mathbf{x}$ since then $s(\pi-\theta;\mathbf{x}^E) = -s(\theta;\mathbf{x}^E)$. This justifies that the asymptotic expansion is pushed to second order in (11). The local approximation to the contribution $KU(\mathbf{x}^E) - J^I$ can be obtained in a similar manner. Its calculation is slightly more complicated since it involves two contributions coming from photons that entered $\mathcal{D}^C$ through Σ^I and Σ^E.

Adding the contributions from the two layer boundaries and sending the thickness of the clear layer to zero (thus identifying $\mathbf{x}^E$ and $\mathbf{x}^I$ with $\mathbf{x} \in \Sigma$), we obtain that

$$KU(\mathbf{x}) = \frac{\partial}{\partial s}\Big(d^C(\mathbf{x})\frac{\partial U}{\partial s}\Big)(\mathbf{x}) - \sigma_a^C(\mathbf{x})U(\mathbf{x}) + \text{ smaller terms.} \tag{15}$$

The diffusion coefficient d^C is positive and the absorption coefficient σ_a^C is non-negative. This implies that the asymptotic limit of the operator K is negative in the sense that neglecting smaller order terms and integrating by parts, $\int_\Sigma (KU)(\mathbf{x})U(\mathbf{x})dS(\mathbf{x}) \leq 0$ for smooth functions $U(\mathbf{x})$, where $dS(\mathbf{x})$ is the surface measure on Σ.

The above procedure can be generalized to the three dimensional case without any theoretical difficulty, although the local parameterization of the surfaces Σ^E and Σ^I and the calculation of the travel times $t(\mathbf{x},\theta,\phi)$ and currents in (10) become more complicated.

3.4 Tangential diffusion coefficient for circular layers.

In the rest of this paper, we assume that the surface Σ is a circle of radius R in two space dimensions $n = 2$ and a sphere of radius R in three space dimensions $n = 3$; see Fig. 2. We also assume to simplify that the clear layer is non-absorbing, i.e. $\sigma_a(\mathbf{x}) = 0$ in $\mathcal{D}^C$. We then obtain that

$$KU(\mathbf{x}^E) = d^C\Delta_\perp U(\mathbf{x}^E) + \text{ small terms,} \tag{16}$$

where $\Delta_\perp$ is the Laplace-Beltrami operator for the sphere when $n = 3$ (i.e., the Laplace operator in the tangent plane to the sphere) and $\Delta_\perp = \frac{\partial^2}{\partial s^2}$ for the circle when $n = 2$. The diffusion coefficient is given in two space dimensions by

$$\begin{aligned} d^C &= d^C_{\mathrm{ex-ex}} + d^C_{\mathrm{ex-in}} + d^C_{\mathrm{in-ex}}, \\ d^C_{\mathrm{ex-ex}} &= \frac{1}{2\pi}\int_0^{\theta_0} \sin\theta (R+L)^2 (2\theta)^2 d\theta \\ d^C_{\mathrm{ex-in}} &= \frac{1}{2\pi}\int_{\theta_0}^{\pi/2} \sin\theta (R-L)^2 \Big(\theta - \arccos\Big(\frac{R+L}{R-L}\cos\theta\Big)\Big)^2 d\theta \\ d^C_{\mathrm{in-ex}} &= \frac{1}{2\pi}\int_0^{\pi/2} \sin\theta (R+L)^2 \Big(-\theta + \arccos\Big(\frac{R-L}{R+L}\cos\theta\Big)\Big)^2 d\theta. \end{aligned} \tag{17}$$

Here, θ_0 is the limiting angle below which incident particles enter the clear layer through the upper surface and exit it through the same upper surface. It is defined by

$$\theta_0 = \arccos\Big(\frac{R-L}{R+L}\Big). \tag{18}$$

The three components of d^C are the contributions of photons that exit (enter) the clear layer through the upper (upper) surface ($d^C_{\mathrm{ex-ex}}$), the upper (lower) surface ($d^C_{\mathrm{ex-in}}$), and the lower (upper) surface ($d^C_{\mathrm{in-ex}}$), respectively. Thus $d^C_{\mathrm{in-ex}}$ is given by $d^I(\mathbf{x}^E)$ in (14) and the two other contributions correspond to the photons crossing the clear layer through Σ^E.

A similar expression can be calculated for the tangential diffusion coefficient in three space dimensions. We have not reproduced this lengthy expression here.

3.5 Generalized diffusion model with local interface conditions.

With these approximations, the generalized diffusion model takes then the following form in the limit of vanishing thickness of the clear layer:

$$\begin{aligned} &-\nabla\cdot D(\mathbf{x})\nabla U(\mathbf{x}) + \sigma_a(\mathbf{x})U(\mathbf{x}) = S(\mathbf{x}) \qquad \text{in } \mathcal{D}\backslash\Sigma \\ &U(\mathbf{x}) + nL_n D(\mathbf{x})\boldsymbol{\nu}(\mathbf{x})\cdot\nabla U(\mathbf{x}) = g(\mathbf{x}) \qquad \text{on } \partial\mathcal{D} \\ &U(\mathbf{x}^+) = U(\mathbf{x}^-) \qquad \text{on } \Sigma \\ &\boldsymbol{\nu}(\mathbf{x})\cdot D(\mathbf{x}^+)\nabla U(\mathbf{x}^+) - \boldsymbol{\nu}(\mathbf{x})\cdot D(\mathbf{x}^-)\nabla U(\mathbf{x}^-) = d^C \Delta_\perp U(\mathbf{x}) \text{ on } \Sigma. \end{aligned} \tag{19}$$

For $\mathbf{x}\in\Sigma$, we have defined $\mathbf{x}^\pm = \mathbf{x} \pm 0\boldsymbol{\nu}(\mathbf{x})$. This equation is much simpler to solve than (9) because the jump conditions are now *local* on Σ. Notice that we have replaced $\mathbf{x}^E$ and $\mathbf{x}^I$ by $\mathbf{x}$ since the layer is sufficiently thin. Also the diffusion equation is now posed on $\mathcal{D}\backslash\Sigma$ instead of $\mathcal{D}\backslash\mathcal{D}^C$. The flux of photons $U(\mathbf{x})$ is continuous across the interface Σ. The current $\boldsymbol{\nu}\cdot\nabla U$ is however discontinuous and its jump is given by $d^C\Delta_\perp U(\mathbf{x})$, which is also continuous since only derivatives along the interface Σ are considered.

The numerical implementation of (19) is also relatively straightforward. Indeed let us consider the variational formulation of (19). Upon multiplying (19) by a test function $w(\mathbf{x})$ and integrating by parts using the Gauss formula, we obtain that

$$\begin{aligned} &\int_{\mathcal{D}} \Big(D(\mathbf{x})\nabla U(\mathbf{x})\cdot\nabla w(\mathbf{x}) + \sigma_a(\mathbf{x})U(\mathbf{x})w(\mathbf{x})\Big)d\mathbf{x} \\ + &\int_\Sigma d^C \nabla_\perp U(\mathbf{x})\cdot\nabla_\perp w(\mathbf{x}) dS(\mathbf{x}) \;+\; \int_{\partial\mathcal{D}} \frac{1}{nL_n} U(\mathbf{x})w(\mathbf{x})dS(\mathbf{x}) \\ = &\int_{\mathcal{D}} S(\mathbf{x})w(\mathbf{x})d\mathbf{x} \;+\; \int_{\partial\mathcal{D}} \frac{1}{nL_n} g(\mathbf{x})w(\mathbf{x})dS(\mathbf{x}). \end{aligned} \tag{20}$$

Here $\nabla_\perp$ is the gradient operator along the surface Σ and dS is the surface measure on Σ and $\partial\mathcal{D}$. Since the diffusion coefficients $D(\mathbf{x})$ and $d^C(\mathbf{x})$ are positive, we obtain that the above equation is well-posed. Moreover its discretization by finite element method (Galerkin projection) is straightforward thanks to the variational formulation (20) [29]. A similar variational formulation was also used to solve (9) [22]. Notice that (19) is however considerably simpler to solve as the calculation and integration of the response operator $\mathcal{R}^C_1$ in (10) is replaced by a single tangential diffusion coefficient d^C.

3.6 Remarks on the mathematical model.

The derivation of (19) can be justified rigorously by using the asymptotic expansions and techniques developed in an earlier work [23]. We present the main results below and refer to that work for additional details.

Denoting by ε the mean free path, i.e., the main distance of propagation of the photons between successive collisions, the scaling of the clear layer such that the operator KU is of order $O(1)$ is given by $L^2|\ln L| \approx \varepsilon$. Discarding logarithmic terms, this means that the clear layer must be approximately of size $\sqrt{\varepsilon} \gg \varepsilon$. When the clear layer is much smaller than $\sqrt{\varepsilon}$, the guiding effects can be neglected as a first approximation and classical diffusion equations (4) are asymptotically valid. When the clear layer is much larger than $\sqrt{\varepsilon}$, it is too large for the diffusion equilibrium $U(\mathbf{x}^E) = U(\mathbf{x}^I)$ to hold. In effect, a nonlocal equilibrium arises, which imposes that the flux of photons is asymptotically constant inside the layer. This case was analyzed [22, 23] both theoretically and numerically.

When the clear layer has the correct scaling, $L^2|\ln L| \approx \varepsilon$, and the curvature of the surface Σ is uniformly positive (is a uniformly positive definite matrix in three space dimensions), we can show [23] that the error between $u(\mathbf{x}, \mathbf{\Omega})$ and $U(\mathbf{x})$ is of order $\sqrt{\varepsilon}$. The error is no longer of order ε as in the case of classical diffusion [10]. For typical mean free paths of order 10^{-3}-10^{-2}, the error will therefore possibly be of the order of a few percents. To further quantify this error term, we propose several numerical simulations in the following section.

When the clear layer is no longer scattering-free, the distance traveled by the photons when they cross the clear layer decreases as fewer photons travel collision-less parallel to the layer boundary. This implies that the tangential diffusion coefficient also decreases. However the final form of the generalized diffusion equation is not modified by weakly scattering layers. In the limit of strongly scattering layers, the tangential diffusion coefficient vanishes. This simply corresponds to the validity of classical diffusion, where the interface conditions are continuity of the flux intensity and current.

More general geometries such as oscillatory clear layers can also be considered [13]. Oscillations will also reduce the value of the tangential diffusion coefficient as photons are forced to exit the clear layer more rapidly by the geometry. Although further theoretical and numerical studies are necessary to adapt the proposed method to more complex geometries, we believe that the tangential diffusion process is a rather stable limiting process to model the guiding effect in clear and not-so-clear layers. All we have to do is to find an average surface Σ and then the tangential diffusion coefficient that generalizes (14).

Let us finally mention that we restrict ourselves here to the steady-state transport equation with isotropic scattering. The generalization of the results presented below to anisotropic scattering is straightforward as long as the diffusion approximation can be justified. Time dependent and frequency harmonic equations also can be treated similarly so long as the variations in time of the source terms are slow compared with the characteristic mean free time, i.e., the mean time between successive collisions of the photons with the underlying medium. For time dependent equations, the term $c^{-1}\frac{\partial u}{\partial t}$ need be added in front of (1), (4), and the main result (19). In the time harmonic case, $c^{-1}i\omega u$ is added instead. Here c is the light speed and ω the modulation frequency of the source term.

4 Numerical simulations

In this section we solve (19) numerically and compare its solution to the transport solution $u(\mathbf{x}, \mathbf{\Omega})$ obtained by a Monte Carlo algorithm. Numerical simulations are performed both for the two and three dimensional problems with circular and spherical clear layers, respectively.

We assume that $S(\mathbf{x}) = 0$ and that $g(\mathbf{x}) = \delta(\mathbf{x} - \mathbf{x}_0)$, where $\mathbf{x}_0 \in \partial\mathcal{D}$ is a point on the boundary of the domain where a constant source emits light isotropically. The transport and diffusion solutions are compared by looking at the exiting currents at the boundary of the domain $\partial\mathcal{D}\backslash\{\mathbf{x}_0\}$. The transport and diffusion currents are given by

$$J_T(\mathbf{x}) = \int_{S^{n-1}} \mathbf{\Omega} \cdot \boldsymbol{\nu}(\mathbf{x}) u(\mathbf{x}, \mathbf{\Omega}) d\mu(\mathbf{\Omega}), \quad J_D(\mathbf{x}) = D(\mathbf{x}) \boldsymbol{\nu}(\mathbf{x}) \cdot \boldsymbol{\nabla} U(\mathbf{x}), \tag{21}$$

respectively. These currents correspond to the information that is available in physical experiments.

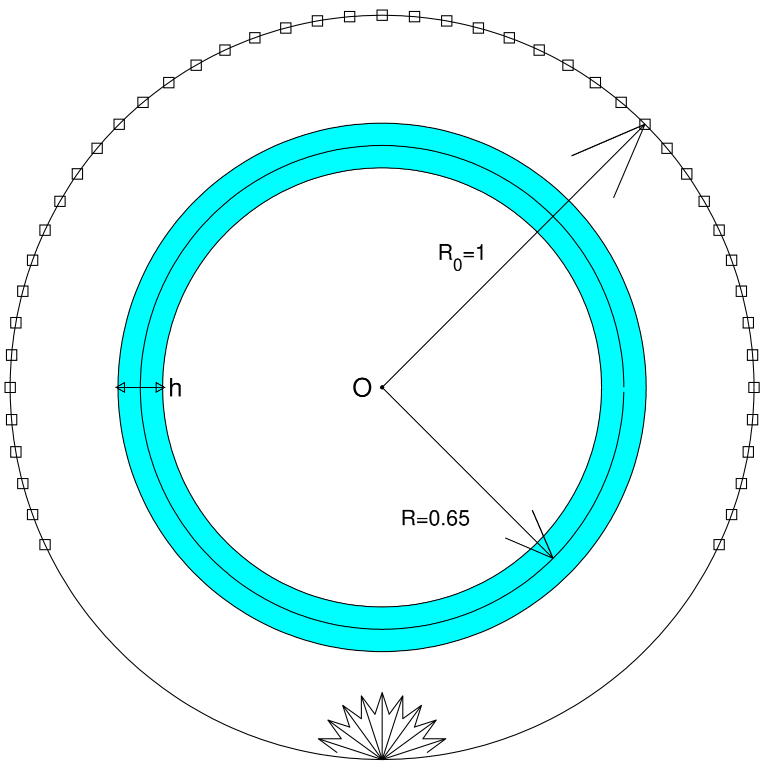

Figure 2: Geometry of the two-dimensional setting and cross-section of the geometry of the three-dimensional setting with azimuthal symmetry.

4.1 Two dimensional numerical simulations.

In two space dimensions, the domain $\mathcal{D}$ is the unit disc $\mathcal{D} = \{\mathbf{x} \in \mathbb{R}^2, |\mathbf{x}| < 1\}$. The surface Σ modeling the clear layer is a circle of radius R. Photons enter the domain at the point $\mathbf{x}_0 = (0, -1)$. In the numerical experiments we have chosen $R = 0.65$. The thickness of the clear layer is given by $h = 2L$; see Fig. 2. We consider several values of h. The scattering cross section $\sigma_s(\mathbf{x})$ is chosen constant and equal to 10^2 in $\mathcal{D}\backslash\mathcal{D}^C$ and vanishes in $\mathcal{D}^C$. This implies that the total size of the domain is of the order of 100 mean free paths. In all our simulations the mean free path is 0.01. We assume that there is no absorption to simplify. In the absence of clear layer, the problem would be very much in the regime of validity of diffusion.

The transport equation (1) is solved by Monte Carlo method [30]. Particles start at $\mathbf{x}_0$ with uniformly chosen initial direction and propagate inside the domain until they exit it. The outgoing current J_T is calculated accordingly. A number of particles of $8\,10^7$ has been used to obtain a sufficiently small statistical variance.

The generalized diffusion model (19) is solved by Fourier decomposition after passage to polar coordinates. The jump of derivatives at the clear layer can easily be accounted for in this setting. We thus obtain a quasi-analytic expression for J_D. This is the reason why we have chosen circular clear layers.

The current at the domain boundary is discretized into 2×36 cells of size 5 degrees each (or $\pi/36$). Cell 1 corresponds to the vicinity of the source and cell 36 corresponds to the vicinity of the upper point $(0, 1)$. The symmetry about $x = 0$ is used in the calculations. The number of particles is such that at least $15\,10^3$ particles exit though each cell. This ensures a statistical relative error of less than 10^{-2} by the law of large numbers, which is below or comparable to the error expected from the diffusion model for a mean free path of 10^{-2}. The lowest density is obviously obtained in the upper cell 36 and in the absence of clear layers. The corresponding diffusive flux is obtained by averaging the flux given by the Fourier expansion in each cell.

We now compare the transport and diffusion exiting currents of photons for several sizes of the clear layer. The thickness of the clear layer varies between 1 and 7 mean free paths. According to theory clear layers of the order of the mean free path are too small to significantly modify the solution obtained in the absence of clear layer. Clear layers on the order of the square root of the mean free path (10 here) however have a significant effect on the solution. Because the mean free path here is still relatively large (in the sense that its square root is not very small) we start seeing effects for clear layers of roughly $2-3$ mean free paths.

h	0.01	0.02	0.03	0.04	0.05	0.06	0.07
$d^C_{\mathrm{ex-ex}}$	0.0064	0.026	0.058	0.10	0.16	0.23	0.32
$d^C_{\mathrm{in-ex}}$	0.0029	0.0093	0.018	0.028	0.039	0.051	0.062
$d^C_{\mathrm{in-in}}$	0.0031	0.011	0.021	0.036	0.053	0.073	0.096
d^C_{theory}	0.0124	0.0455	0.0971	0.166	0.253	0.355	0.475
$d^C_{\mathrm{best\ fit}}$	0.0129	0.0465	0.0983	0.167	0.253	0.356	0.474
E_{GDM} (%)	1.17	1.56	1.43	1.09	0.81	0.56	0.60
E_{BF} (%)	0.73	0.65	0.57	0.49	0.46	0.47	0.46
E_{DI} (%)	3.3	10.2	17.7	24.5	30.2	35.3	39.8
E_{DI2} (%)	5.7	11.8	18.2	17.8	18.1	17.9	17.8

Table 1: Tangential diffusion coefficients and relative root mean square error (L^2 norm) between the Monte Carlo simulations and the various diffusion models for several thicknesses of the clear layer. The errors E_{GDM}, E_{BF}, E_{DI}, and E_{DI2} represent the relative root mean square error (in percentage) between the Monte Carlo simulations and the generalized diffusion model obtained using d^C_{theory}, the generalized diffusion model obtained by best fit, the classical diffusion equation, and the generalized diffusion model with tangential diffusion coefficient 1.5 times larger than d^C_{theory}, respectively.

Tab. 1 present the results of the numerical experiments. For thicknesses h between 1 and 7 mean free paths, the tangential diffusion coefficient defined in (17) is given in row 4 and its three components in rows 1 to 3. The coefficient obtained by best fitting (in the least-square sense) the generalized diffusion model to the Monte Carlo data on the outgoing density between angles 60 and 180 (cells 12 to 36) is given in row 5. We observe that the theoretical coefficient is quite close to the best fit. This is confirmed by looking at the errors made by the different models. The relative L^2 norm between the Monte Carlo simulations and the various models between cells 12 and 36 is given in rows 6 to 9 for the generalized diffusion model, the best fit from data, the classical diffusion model with no clear layer (i.e., the diffusion coefficient is taken constant and equal to 1/200 on the whole domain), and a generalized diffusion model where the tangential diffusion coefficient has been chosen very large, respectively. By very large, we mean a tangential diffusion coefficient 1.5 times larger than its theoretical value. This solution corresponds to overestimating the guiding effect of the clear layer as we would obtain by using a diffusion approximation with a large diffusion coefficient given by (5) inside the clear layer. It is known that the correct solution is then not obtained [14, 22, 23, 28, 13]. The different models are also compared in Figure 3 for four different thicknesses h. The viewgraphs confirm the error estimates of Tab. 1.

4.2 Interpretation of results.

Let us first state that the generalized diffusion model successfully deals with the guiding effects caused by the presence of a clear layer. The relative root mean square error between transport and this diffusion model does not exceed two percents. The accuracy degrades in the vicinity of the source term (not shown) but this

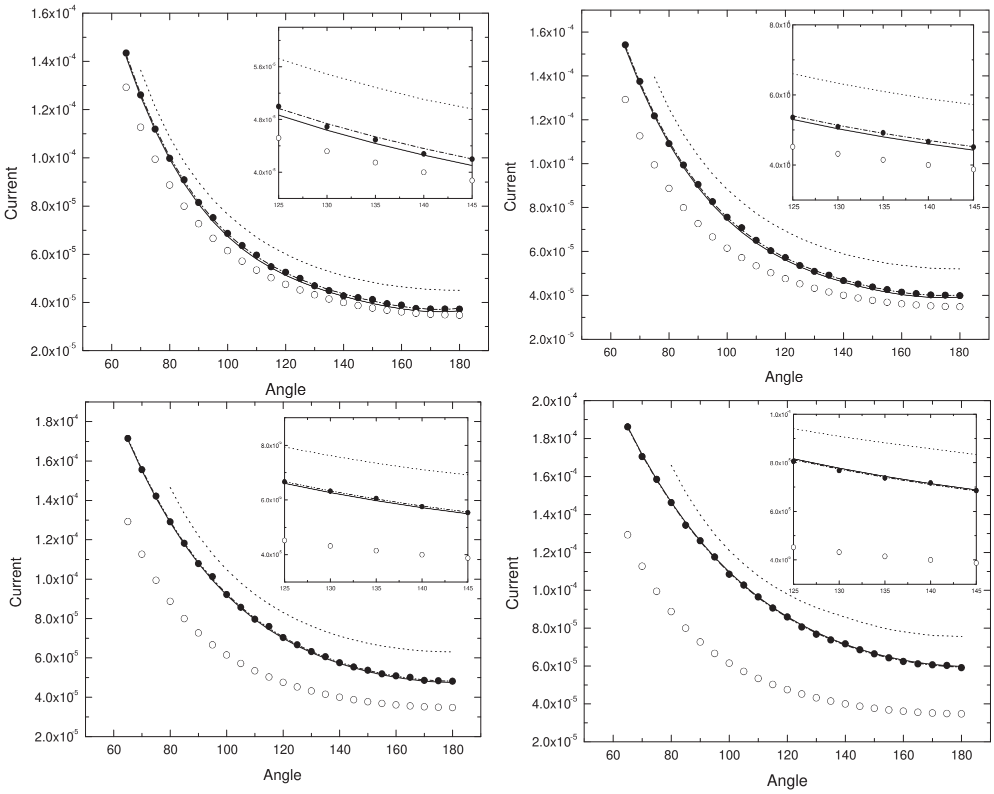

Figure 3: Plots of the current between cells 14 (70 degrees) and 36 (180 degrees) at the boundary of the unit disc (two-dimensional simulation) for the Monte Carlo solution and the different diffusion models. The thickness of the clear layer in mean free path is 2, 3, 5, and 7 for the top-left, top-right, bottom-left, bottom-right figures, respectively. In each sub-figure, the Monte Carlo simulation is represented by solid circles, the classical diffusion by empty circles, the generalized diffusion model with theoretical tangential diffusion coefficient by the sold line, the generalized diffusion model with best fit by the dash-dotted lines, and the generalized model with large tangential diffusion coefficient by the dotted line. The inset represents a magnification of the above results between angles 125 and 145.

is classical of diffusion approximations and is independent of the clear layer. The diffusion model obtained from (17) is almost as accurate as the best fit model. Classical diffusion, where the clear layer is replaced by a diffusive medium, is accurate when the clear layer is thin. However the error becomes unacceptable in practice (about 10%) even for thicknesses of the order of two mean free paths. The guiding effect is neglected and the upward propagation of photons is clearly underestimated. The opposite effect arises when the tangential diffusion coefficient is chosen too large. As we have already mentioned, this is similar to using the diffusion model (5) also inside the clear layer, which gives higher a diffusion coefficient than is physically correct and overestimates the guiding effect.

Let us conclude with a short comment on the theoretical diffusion coefficient. It is not difficult to show that asymptotically as $h \to 0$, $d^C_{\rm ex-ex}$ is a term of order h^2 whereas the other contributions $d^C_{\rm in-ex}$ and $d^C_{\rm in-in}$ are terms of order $h^2|\ln h| \gg h^2$. We have observed this behavior numerically for values of h of order $10^{-4} - 10^{-3}$. However in the cases shown here, where the mean free path is of order 10^{-2}, the term $d^C_{\rm ex-ex}$, although asymptotically smaller than the other contributions, actually dominates in the calculation of the theoretical diffusion coefficient.

4.3 Three dimensional numerical simulations.

Let us now consider the three-dimensional case. The domain is now a sphere of radius 1, the clear layer a corona of thickness h centered at $R = 0.65$, and the source is at position $(0, 0, -1)$. The transport equations are still solved by Monte Carlo method and the diffusion equation by projection onto spherical harmonics.

We did not estimate the theoretical tangential diffusion coefficients that generalizes (17) to the three-dimensional case. This coefficient could certainly be calculated analytically or computed numerically by assessing how far photons can go on average by crossing the clear layer. Rather we would like to stress another advantage we see in (19) as a model in optical tomography, where the photon measurements at the boundary are used to image the diffusion and absorption properties of the domain on the other side of the clear layer (i.e., close to the origin $(0, 0, 0)$). We claim that the clear layer can be modeled by a possibly spatially dependent tangential diffusion coefficient provided that we have an a priori knowledge of its location. In other words we claim that the inverse problem based on simulating the full clear layer (in transport then) and the inverse problem based on replacing the clear layer by a tangential diffusion process (with a priori unknown strength) will give similar reconstructions. This of course comes at the expense of also reconstructing the value of the tangential diffusion coefficient from the measured data. This claim corresponds to showing that the best diffusion fit yields a good approximation to the transport solution. We have seen that this is the case in two dimensions.

We now present results that confirm that this is also the case in three dimensions. The number of particles used in the calculations in $2\,10^7$. Such calculations are already quite long because particles stay longer inside the domain in three dimensions than in two dimensions. Moreover the number of particles exiting the domain in the upper part of the sphere is also smaller than in two dimensions. This renders our numerical simulations less accurate than in two dimensions. This has the advantage at least of mimicking more closely noisy measurements and thus we consider them as an interesting benchmark. The numerical results are presented in Fig. 4. They certainly show that validity of (19) as an accurate model to simulate the guiding effect. The root mean square error between the transport solution and the best fit generalized diffusion model is of the order of $2-3\%$. This error is moreover mostly due to random fluctuations. Other diffusion models that do not correctly account for this effect introduce too large errors to be really considered as practical for the purpose of inversion of physical properties from boundary measurements [13, 14, 22, 23, 28]. For instance classical diffusion is our simulations is as far as 50% off the transport solution.

5 Conclusions

We propose a generalized diffusion model that accounts for the multiple scattering of photons in highly scattering media (classical diffusion regime) and well as for the near-collision-less propagation of the same photons in clear layers (purely transport regime resulting in a guiding effect).

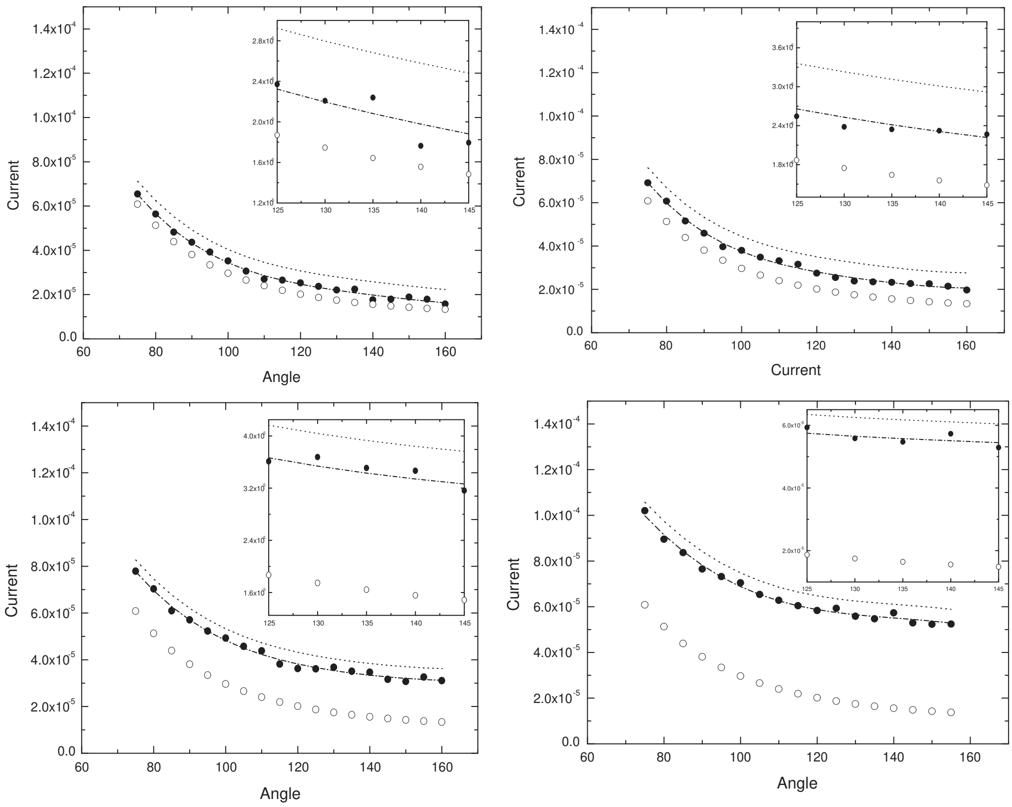

Figure 4: Plots of the current between cells 15 (75 degrees) and 32 (160 degrees) at the boundary of the unit sphere (three-dimensional simulation with azimuthal symmetry) for the Monte Carlo solution and the different diffusion models. The thickness of the clear layer in mean free path is 1, 2, 4, and 6 for the top-left, top-right, bottom-left, bottom-right figures, respectively. In each sub-figure, the Monte Carlo simulation is represented by solid circles, the classical diffusion by empty circles, the generalized diffusion model with theoretical tangential diffusion coefficient by the sold line, the generalized diffusion model with best fit by the dash-dotted lines, and the generalized model with large tangential diffusion coefficient by the dotted line. The inset represents a magnification of the above results between angles 125 and 145.

This model can be mathematically derived from the phase space radiative transport equation as a small mean-free-path limit. It captures the guiding effect of photons in the clear layer quite well. Moreover it has almost the same cost as classical diffusion, which completely fails to model the clear layer effects, and a lower cost than previously derived generalized diffusion equations, which are already much less expensive than full transport solutions. The reason for this lower cost is that the nonlocal interface conditions of the latter diffusion models are replaced by their best local approximation. This best local approximation takes the form of a tangential diffusion process.

The strength of this diffusion process can be calculated analytically or numerically provided that one has access to the geometry of the clear layer. When this geometry is unknown or only partially known, we have shown numerically that the diffusion process that best fits the impact of the clear layer gives boundary measurements that are visually indistinguishable from the measurements obtained by solving the full transport equations. We believe that the generalized diffusion model can thus safely be used in optical tomography as an accurate approximation of the forward model.

It remains to apply the method to the inverse problem [14], which consists of reconstructing $\sigma_a(\mathbf{x})$ and $D(\mathbf{x})$ from boundary measurements. The validation of the method to solve the inverse problem with more general geometries for the clear layer, both for the steady-state equations and for the time-domain or frequency-domain [1] equations, is the object of ongoing research.

Acknowledgment

The authors wish to thank the reviewers for their constructive comments. This research was supported in part by NSF grant DMS-0233549 and by ONR grant N00014-02-1-0089.

References

[1] S.R. Arridge, "Optical tomography in medical imaging," Inverse Problems 15, R41-R93 (1999).

[2] A.Y. Bluestone, G.S. Abdoulaev, C. Schmitz, R.L. Barbour and A.H. Hielscher, "Three-dimensional optical-tomography of hemodynamics in the human head," Optics Express 9, 272-286 (2001).

[3] O. Dorn, "A transport-backtransport method for optical tomography," Inverse Problems 14, 1107-1130 (1998).

[4] V.A. Markel and J.C. Schotland, "Inverse problem in optical diffusion tomography. I. Fourier-Laplace inverse formula," J. Opt. Soc. Am. A 18, 1336-1347 (2001).

[5] V.A. Markel and J.C. Schotland, "Inverse problem in optical diffusion tomography. II. Role of boundary conditions," J. Opt. Soc. Am. A 19, 558-566 (2002).

[6] G.J. Müller (eds.), *Medical Optical tomography: functional imaging and optical technologies*, Series Vol. IS11, SPIE, Bellingham, Wash. (1993).

[7] F. Natterer and F. Wübbeling, *Mathematical methods in Image Reconstruction* (SIAM monographs on Mathematical Modelling and Computation, Philadelphia, 2001).

[8] PIERS2002, Session on Optical Tomography and Optical Imaging, Progress in Electromagnetic Research Symposium (PIERS), July 1-5, Cambridge, Massachusetts, USA (2002)

[9] A.D. Klose and A.H. Hielscher, "Optical tomography using the time independent equation of radiative transfer," J. Quant. Spect. and Rad. Trans. 72, 715-732 (2002).

[10] R. Dautray and J-L. Lions, *Mathematical Analysis and Numerical Methods for Science and Engineering, Vol 6* (Springer-Verlag, Berlin, 1993).

[11] E.W. Larsen and J.B. Keller, "Asymptotic solution of neutron transport problems for small mean free paths," J. Math. Phys. 15, 75-81 (1974).

[12] A.H. Hielscher, R.E. Alcouffe and R.L. Barbour, "Comparison of finite-difference transport and diffusion calculations for photon migration in homogeneous and heterogeneous tissues," Phys. Med. Biol. 43, 1285-1302 (1998).

[13] J. Ripoll, M. Nieto-Vesperinas, S.R. Arridge and H. Dehghani, "Boundary conditions for light propagation in diffuse media with non-scattering regions," J. Opt. Soc. Am. A 17, 1671-1681 (2000).

[14] H. Dehghani, S. R. Arridge, M. Schweiger and D. T. Deply, "Optical tomography in the presence of void regions," J. Opt. Soc. Am. A, 17, 1659-1670 (2000).

[15] S.R. Arridge and J.C. Hebden, "Optical Imaging in Medicine: II. Modelling and reconstruction," Phys. Med. Biol. 42, 841-853 (1997).

[16] C.K. Hayakawa, J. Spanier, F. Bevilacqua, A.K. Dunn, J.S. You, B.J. Tromberg, and V. Venugopalan, "Perturbation Monte Carlo methods to solve inverse photon migration problems in heterogeneous tissues," Optics letters 26(17), 1335-1337 (2001).

[17] G. Bal and Y. Maday, "Coupling of transport and diffusion models in linear transport theory," M2AN 36, 69-86 (2002).

[18] G. Bal and X. Warin, "Discrete ordinate methods in xy-geometry with spatially varying angular discretization," Nuclear Science and Engineering 127, 169-181 (1997).

[19] F. Golse, S. Jin and C.D. Levermore, "The convergence of numerical transfer schemes in diffusive regimes. I. Discrete-ordinate method," SIAM J. Numerical Anal. 36, 1333-1369 (1999).

[20] E.W. Larsen, J.E. Morel and W.F. Miller Jr., "Asymptotic solutions of numerical transport problems in optically thick, diffusive regimes," J. Comp. Phys. 69, 283-324 (1987)

[21] M. Tidriri, "Asymptotic analysis of a coupled system of kinetic equations," C. R. Acad. Sci. Paris, t.328, Série I Math., 637-642 (1999).

[22] G. Bal, "Particle transport through scattering regions with clear layers and inclusions," J. Comp. Phys. 180, 659-685 (2002).

[23] G. Bal, "Transport through diffusive and non-diffusive regions, embedded objects, and clear layers," SIAM J. Appl. Math. 62, 1677-1697 (2002).

[24] M. Choulli and P. Stefanov, "Reconstruction of the coefficients of the stationary transport equation from boundary measurements," Inverse Problems 12, L19-23 (1996).

[25] A. Tamasan, "An inverse boundary value problem in two-dimensional transport," Inverse Problems 18, 209-219 (2002).

[26] G. Bal, V. Freilikher, G. Papanicolaou, and L. Ryzhik, "Wave transport along surfaces with random impedance," Phys. Rev. B 62, 6228-6240 (2000).

[27] J.M. Luck and T.M. Nieuwenhuizen, "Light scattering from mesoscopic objects in diffusive media," Eur. Phys. J. B 7, 483-500 (1999).

[28] M. Firbank, S.A. Arridge, M. Schweiger and D.T. Delpy, "An investigation of light transport through scattering bodies with non-scattering regions," Phys. Med. Biol. 41, 767-783 (1996).

[29] S.C. Brenner and L.R. Scott, *The mathematical theory of finite element methods* (Springer-Verlag, New York, 2002).

[30] J. Spanier and E.M. Gelbard, *Monte Carlo principles and neutron transport problems* (Addison-Wesley, Reading, Mass., 1969).